EXPERIMENTAL STUDY ON INFLUENCE OF FORCED VIBRATION OF COOLING CHANNEL ON HEAT TRANSFER INSTABILITY AT ATMOSPHERIC AND QUASI-CRITICAL PRESSURE

by

Kun LI[a,b], Yuxiang HAN[c], Zhixiong HAN[d], Junlong ZHANG[d*], and Hao ZAN[c]

[a] Chinese Aeronautical Establishment, Beijing, China
[b] Graduate School of Chinese Aeronautical Establishment, Beijing, China
[c] Jiangsu University of Science and Technology, Jiangsu, China
[d] Harbin Institute of Technology, Heilongjiang, China

Original scientific paper
https://doi.org/10.2298/TSCI220918094L

Hydrocarbon fuel is used as coolant to cool scramjet by flowing through cooling channels at atmospheric pressure and quasi-critical pressure conditions. The instability of the heat transfer will occur in this process. However, the effect of scramjet vibration on the heat transfer instability is unclear. In order to study the effect of cooling channel forced vibration on the unstable heat transfer performance at trans-crtical pressure, cooling channel heat transfer characteristics under different vibration condition are analyzed. Experimental results show that at atmospheric pressure, cooling channel vibration causes a drastic change in the temperature of the inner wall during unstable heat transfer process, but vibration will not change the fuel bulk temperature oscillation process. As a result, forced vibration can lead to heat transfer deterioration in the gas-liquid two-phase flow. Under the condition of quasi-critical pressure, cooling channel vibration not only change the inner wall temperature, but also influence the fuel bulk temperature. The forced vibration can lead to heat transfer enhancement. High frequency vibration can effectively suppress heat transfer instability and reduces heat transfer fluctuations.

Key words: *cooling channel, atmospheric pressure, quasi-critical pressure, vibration, heat transfer*

Introduction

Hydrocarbon fuel is widely used as regenerative coolant in scramjets [1]. Before injected into the combustor, hydrocarbon fuel is forced into the cooling passage distributed in the hot wall of combustor for absorbing heat. There are many problems in hydrocarbon fuel cooling technology [2]. For example, one of the main problems is the heat transfer instability due to physical property changes at critical pressure [3]. Large fluctuations in temperature have been observed in hydrocarbon fuel. This problem has significant influences on the safe operation of a scramjet. Unstable flow conditions of fuel in regenerative cooling channels can cause critical failure in thin-walled test sections, because the flow oscillations can cause the tube to resonate when the natural frequency is matched [4].

* Corresponding author, e-mail: junlongzhang1990@163.com

Fuel flow instability may probably be induced by complex and variable working conditions during cooling process [5]. On one hand, the working pressure of fuel should be kept above the critical pressure to avoid two-phase flows and heat transfer deterioration caused by boiling during cooling process. On the other hand, hydrocarbon fuel is heated to as high as 800 °C to satisfy the cooling demands. Such a wide range of changes in fuel temperature will cause a significant change in the properties of fuel [6]. A number of unstable phenomena have been obtained experimentally and numerically [7, 8]. For example, Kafengauz [9] observed that the heat transfer with pseudo-boiling at $P > P_{\rm cr}$ and surface boiling at $P < P_{\rm cr}$ was always accompanied by pressure oscillations. Linne *et al.* [10] conducted a series of heat transfer experiments of JP-7, and found that the instability of fuel flow occurs in all the tests at supercritical pressure, supercritical wall temperature, and a subcritical bulk fluid temperature. Alad'ev [11] measured the size and wavelength of sound velocity when *n*-heptane produces acoustic oscillations under supercritical pressure. The effect of heat flux on pressure fluctuations produced by acoustic oscillations is analyzed in the heat transfer experiment of supercritical flow of toluene [12, 13]. Zhu *et al.* [14] found a transition unstable oscillation phenomenon in the flow heat transfer experiment of *n*-decane under supercritical pressure. Edwards [15] found that the flow oscillation was caused by nucleoid boiling near the inner wall of the tube. Hines *et al.* [16] observed periodic pressure oscillations accompanied by a strong screeching sound in the heat transfer study of RP-1 aviation kerosene. Liu *et al.* [27] found flow instability, pressure drop deduction, and heat transfer deterioration happened simultaneously accompanied with acoustic flow instability and diabatic pressure drop deduction in the critical region. Zhou *et al.* [18] experimental studied the instability of supercritical hydrocarbon fuel flow near the critical temperature region and cracking temperature region, and concluded that fuel density relative change rate was the primary factor which caused the instability of the system. In reference [19, 20], the onset of flow instability in overheated fluids was very often associated with non-linear boiling waves formation.

Due to the thin-walled structure, the scramjet needs to withstand huge aerodynamic loads and aerodynamic thermal loads [21]. The cooling channels embedded in wall are affected by vibration under the action of supersonic airflow [22]. There are a lot of studies about the influence of vibration on the heat transfer of tube [23, 24]. Despite the existing results, there are still significant challenges in the study of heat transfer instability of hydrocarbon fuel flow. In particular, our previous research found that the forced vibration of cooling channel could suppress the instability of heat transfer at supercritical pressure [2]. This result shows that the external vibration has an effect on the heat transfer process of the hydrocarbon fuel in the cooling channel. However, the effect of forced vibration on the heat transfer instability at trans-crtical pressure is unclear. In order to study the effect of cooling channel forced vibration on the unstable heat transfer characteristics at trans-crtical pressure, cooling channel heat transfer performance under different vibration parameters condition is analyzed in this paper.

Experimental system and data processing

Experimental system

The tests were conducted in Harbin Institute of Technology. The experiments of heat transfer instability have been conducted in horizontal circular tubes with different conditions (as shown in fig. 1). The main test section and pre-heater were stainless steel tubes which were heated by alternating current and thermally insulated by a layer of aluminum silicate fiber, with corrections for the heat losses. The test pressure is divided into atmospheric pressure (0.1 MPa) and quasi-critical pressure (3 MPa). The RP-3 kerosene is used as the working substance for the experiment.

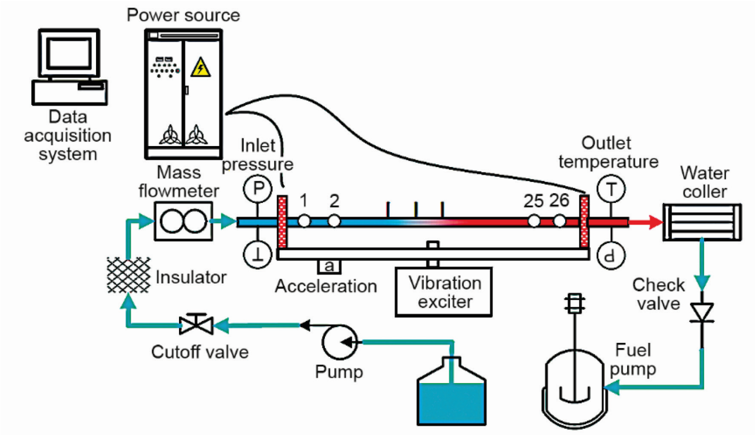

Figure 1. Schematic diagram of the experimental set-up

Some parameters are measured per second using Nl c-rio data acquisition system. The sampling frequency range is 100 Hz. The outlet temperature refers to the outlet fluid temperature measured by *K*-type armored thermocouples. Pressure sensors are installed in the inlet/outlet test section and the fuel sump. The inlet pressure refers to the inlet fluid pressure measured by the pressure sensor. Coriolis flow meters are installed at the inlet of the tube to measure the mass-flow rate. The response time of the pressure sensor (MPM489) and armored thermocouples is 2 ms and 0.5 seconds, respectively. The RP-3 includes 52.44% alkanes, 7.64% alkenes, 18.53% benzenes, 15.54% cycloalkanes, 4.39% naphthalenes, and 1.46% other components [25]. The critical pressure of RP-3 is 2.34 MPa, and critical temperature is 645 K. The specifications of the apparatuses and the uncertainties of measurements are shown in tab. 1. The vibration exciter of DH40100 is manufactured by Donghua Testing Technology. It has a maximum excitation force of 100 N and frequency range between 0.1 Hz and 2.5 kHz. The heating section is fixed to restrict its movement in other directions.

Table 1. The specifications of the apparatuses

Apparatuses	Operation range	Accuracy	Brand	Uncertainty
Mass-flow rate	1-1.5 g/s	±0.5%	Ningbo Kio (KF-500)	±1.0%
Pressure	0-3 MPa	±0.5%	Micro (MPM489)	±0.65%
Temperature	0-1260 ℃	±1℃	Omega (K-type)	±0.58%

Data processing

The local heat transfer coefficient and Nusselt number were calculated:

$$h_x = \frac{q_x}{T_{\mathrm{w}x,\mathrm{in}} - T_{\mathrm{b},x}} \tag{1}$$

where $T_{\text{w}x,\text{in}}$ is the inner wall temperature, $T_{\text{b},x}$ – the bulk fluid temperature, d_i – the inner diameter, and λ_x – the thermal conductivity at the bulk fluid temperature. The local heat flux was calculated from the measured current and the resistivity:

$$q_x = \frac{4I^2 \rho_x}{\pi d_\text{in}(d_\text{out}^2 - d_\text{in}^2)} - q_{\text{loss},x} \tag{2}$$

The resistivity, ρ_x, of the stainless steel is a function of the local outer-wall temperature, $T_{\text{wo},x}$. The local heat dissipation density, $q_{\text{loss},x}$, is related to the surface characteristics and size of the heat dissipation surface and the temperature difference with the environment.

The thermal differential equation of tube is:

$$\frac{1}{r}\frac{\partial}{\partial r}\left(\lambda_\text{s} r \frac{\partial T}{\partial r}\right) + \dot{\Phi} = 0 \tag{3}$$

$$\dot{\Phi} = \frac{I^2 R(T)}{\pi^2 (r_\text{out}^2 - r_\text{in}^2)} \tag{4}$$

where λ_s is the thermal conductivity of stainless steel, R – the electric resistance, I – the ellectric current, and $\dot{\Phi}$ – the volumetric heat source. The boundary conditions are such that when $r = r_\text{out}$, $T = T_{\text{wo},x}$ and $\lambda_\text{s}(\partial T)/(\partial r) = -q_{\text{loss},x}$. Therefore, the inner wall temperature is obtained by integrating from r_in to r_out. The formula for calculating the inner wall temperature is:

$$T_{\text{w}x,\text{in}} = \frac{\left(T_{\text{w}x,\text{out}} - \dot{\Phi}\frac{r_\text{out}^2}{2} - q_{x,\text{loss}} r_\text{out}\right)\ln\frac{r_\text{out}}{r} - \frac{\dot{\Phi}}{4}(r_\text{out}^2 - r_\text{in}^2)}{\lambda_\text{s}} \tag{5}$$

The heat dissipation capability of the pipe to the surrounding air can be calibrated by the air heating experiment. The fitting curve can be expressed in the form of a polynomial function. This heat loss calculation method has been widely used by published studies:

$$\dot{q}_\text{loss}(T_\text{wo}) = \frac{UI}{A_{j\text{h}}} = a(T_\text{wo} - T_0)^3 + b(T_\text{wo} - T_0)^2 + c(T_\text{wo} - T_0) + d \tag{6}$$

where $\dot{q}_\text{loss}(T_\text{wo})$ is the heat flux density of the heat dissipation loss of the heating pipe, T_wo – the temperature of the outer wall of the pipe, $A_{j\text{h}}$ – the outer surface area of the heating pipe, and T_0 – the ambient temperature. Fitting curve is performed with the total heat sink of the fuel along the entire pipe length and the fuel outlet temperature can be obtained:

$$\dot{Q}_\text{total} = f(\overline{T}_\text{out}) = a\overline{T}_\text{out}^4 + b\overline{T}_\text{out}^3 + c\overline{T}_\text{out}^2 + \text{d}\overline{T}_\text{out} + e \tag{7}$$

where $\overline{T}_\text{out}$ is the outlet fuel temperature of the heating section. The fuel average temperature in the pipe can be inverse calculated according to the heat sink at a certain local position:

$$\overline{T}_\text{b} = f^{-1}(\dot{Q}_\text{total}) \tag{8}$$

Experimental results and analysis

Basic heat transfer characteristics

In the study of this section, the working conditions used are: fluid inlet temperature 293 K, system pressure 0.1 MPa, mass-flow rate 1 g/s, heat flux of 90 kW/m^2, 120 kW/m^2, and 150 kW/m^2, respectively. When the heat flux is 90 kW/m^2, it is found that the fuel temperature and the wall temperature oscillate regularly, and when the heat flux is 120 kW/m^2 and 150 kW/m^2, it is found that the fuel temperature and the wall temperature return to stability. Figure 2 shows the variation of the temperature of the inner wall of the pipe wall along the flow direction. It can be seen from the figure that the wall temperature when the heat flux density is 90 kW/m^2 oscillates is significantly different from the wall temperature of 120 kW/m^2 and 150 kW/m^2. When the heat flux density is 90 kW/m^2, the inner wall temperature keeps rising steadily along the flow direction, rising from 390 K to 490 K. When the heat fluxes are 120 kW/m^2 and 150 kW/m^2, the inner wall temperature starts to rise steadily, and then there is a sharp rise process. The sharp rise position of the wall temperature with the heat flux of 150 kW/m^2 is closer to the front than the position of 120 kW/m^2, and the temperature of the wall temperature rise is larger than that of 120 kW/m^2. Figure 3 shows the variation of fuel temperature along the flow direction. When the fuel temperature is heated to 446 K, the heating will not continue to increase the temperature of fuel. The length of the fuel that remains stable in the channel decreases sequentially when the heat fluxes are 90 kW/m^2, 120 kW/m^2 and 150 kW/m^2.

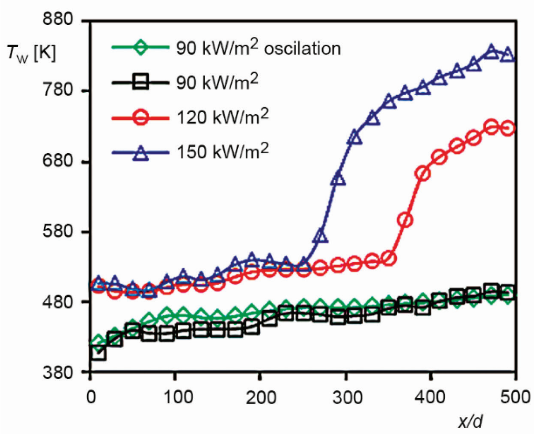

Figure 2. Variations of inner wall temperature

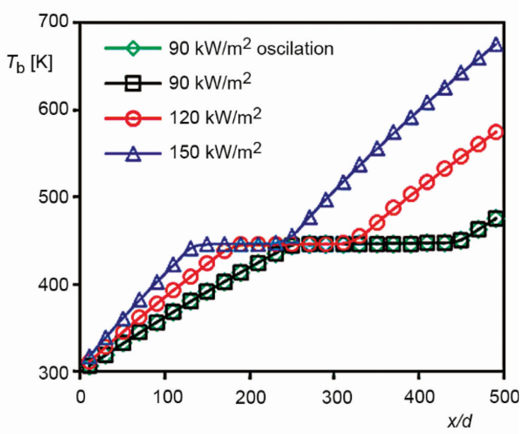

Figure 3. Variations of fuel temperature

Figures 4 and 5 describe the variation of the heat transfer coefficient and Reynolds number along the flow direction, respectively. Compared with boiling heat transfer but no oscillation, the heat transfer system during boiling oscillation can be divided into three parts. When *x*/*d* is less than 300, there is obvious heat transfer enhancement phenomenon. When *x*/*d* is greater than 300 but less than 440, there is obvious heat transfer deterioration. When *x*/*d* is greater than 440, the phenomenon of heat transfer enhancement occurs again. When the heat fluxes are 120 kW/m^2 and 150 kW/m^2, the heat transfer coefficient has experienced a process of increasing, stable, decreasing, and then stable.

In order to further study the unsteady flow phenomenon in the quasi-critical region, the working conditions used in this section are: fluid inlet temperature 293 K, system pressure

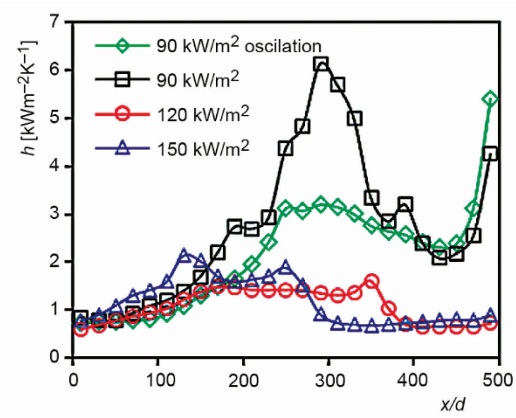

Figure 4. Variations of heat transfer coefficient

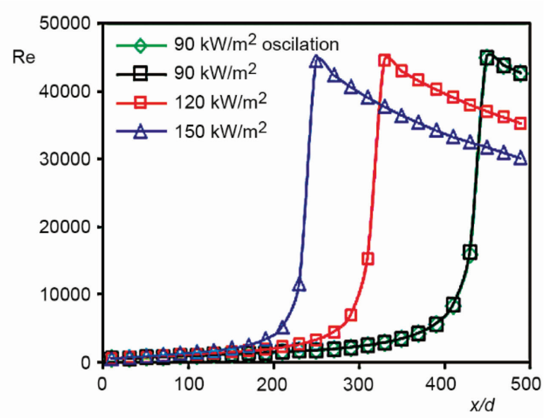

Figure 5. Variations of fuel Reynolds number

3 MPa, mass-flow rate 1.5 g/s, and heat fluxes of 60 kW/m^2 and 90 kW/m^2, respectively. When the heat flux is 90 kW/m^2, the phenomenon of fuel temperature oscillation, wall temperature oscillation, pipeline vibration accompanied by sharp metal hammering sound was observed. Figure 6 shows the variation of the outlet fuel temperature with time, the dotted line represents the trans-critical temperature of RP-3 aviation kerosene at 3 MPa, it can be seen from the figure that the outlet fuel temperature oscillates around the quasi-critical temperature. Figure 7 describes the temperature changes of the pipeline at three positions of $x/d = 100$, $x/d = 300$, and $x/d = 500$, which can reflect the overall temperature change of the pipeline. The fluctuation amplitude of the wall temperature at $x/d = 100$ is smaller than those at $x/d = 300$ and $x/d = 500$. The overall fluctuation phase of the three positions is basically the same, and the overall wall temperature of the pipeline is greater than the quasi-critical fuel temperature.

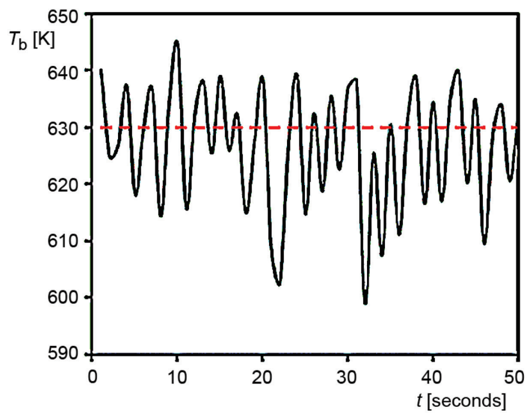

Figure 6. Diagram of fuel bulk temperature

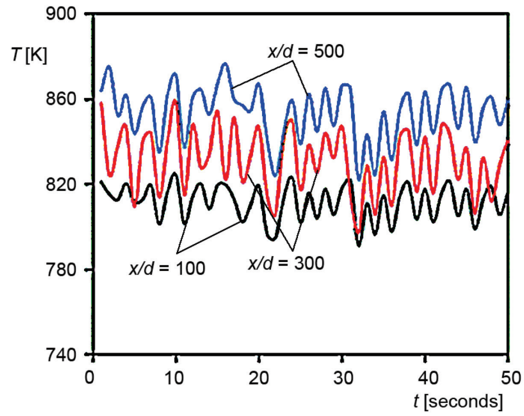

Figure 7. Diagram of wall temperature

The outlet fuel temperature oscillates around the quasi-critical temperature, and the main flow temperature in the pipe is generally lower than the quasi-critical temperature. The near-wall fluid temperature is approximately expressed by the pipe wall temperature. The physical properties of the near-wall fluid and the outlet fluid undergo drastic changes. Figure 8 depicts the changes in fluid density, viscosity, specific heat capacity and thermal conductivity at the outlet main flow and near the wall with $x/d = 300$. Among the four thermophysical parameters, specific heat capacity and thermal conductivity are related to heat transfer, which respectively characterize the ability of fluid to absorb and transfer heat.

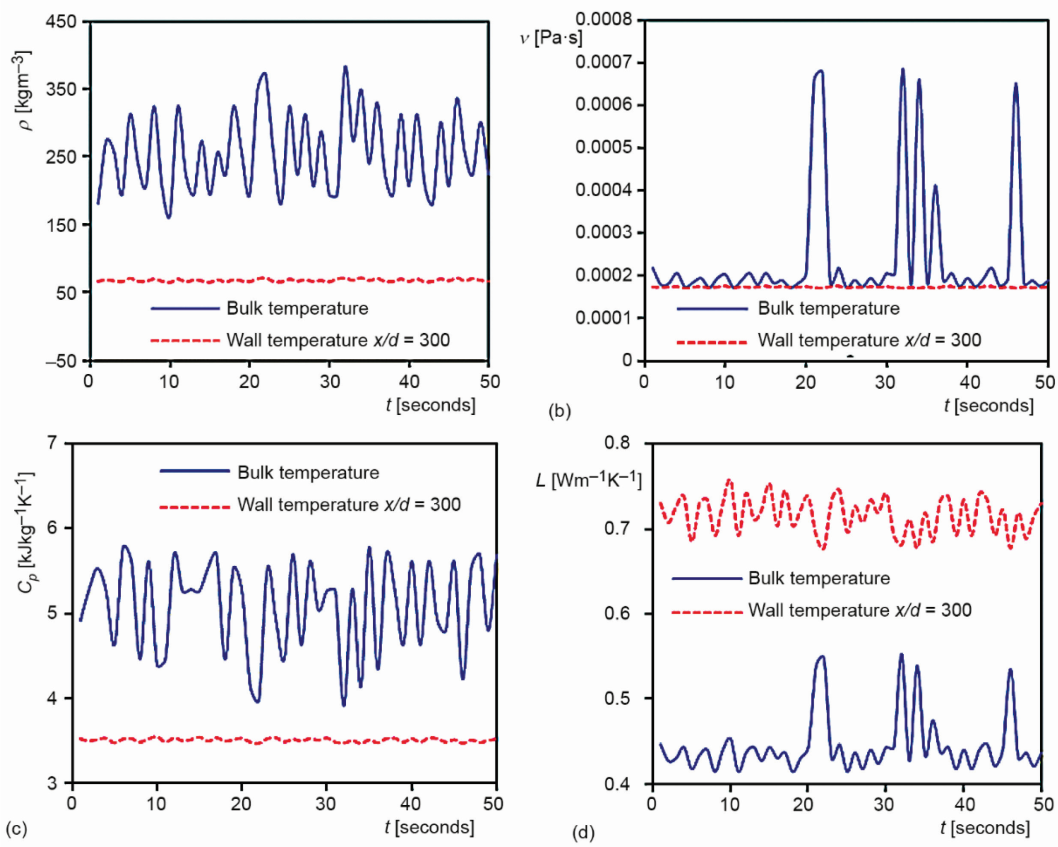

Figure 8. Variations of fuel thermophysical properties

Influence of vibration on unstable heat transfer at atmospheric pressure

The boiling oscillation occurs when the experimental condition is the pressure of 0.1 MPa, the heating power of 90 kW/m^{2}K, the flow rate of 1 g/s, and the inlet temperature of 293 K. The fuel temperature fluctuation of cooling channel affected by forced vibration is shown in fig. 9. During the process of boiling heat transfer, vibrations of different frequencies are applied to the channel, and the vibration data are represented by blue lines. Axial vibration with a frequency of 10 Hz and an amplitude of 20 m/s^2 was applied between 250 seconds and 285 seconds. Vibration with a

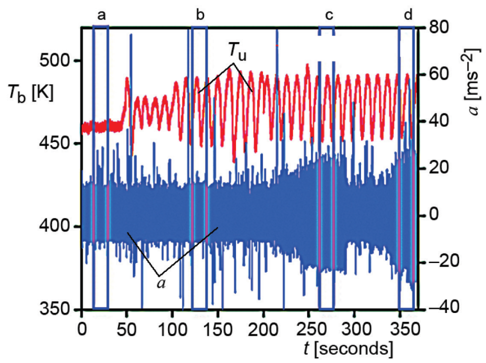

Figure 9. Variations of fuel specific heat capacity along the flow direction

frequency of 50 Hz and an amplitude of 20 m/s^2 was applied between 340 seconds and 370 seconds. The amplitude and frequency of the fuel temperature fluctuation did not change, which means that the vibration did not change boiling oscillation process.

The boiling oscillation process can be divided into four stages, as shown in fig. 10, a represents entering the boiling heat transfer state but no boiling oscillation phenomenon, and no external vibration is applied. Figure 10(b) represents the boiling oscillation state, and no external vibration is applied. Figure 10(c) represents the boiling oscillation state and external axial vibration with a frequency of 10 Hz and an amplitude of 20 m/s^2 exists. Figure 10(d) represents the boiling oscillation state and external axial vibration with a frequency of 50 Hz and an amplitude of 20 m/s^2 exists.

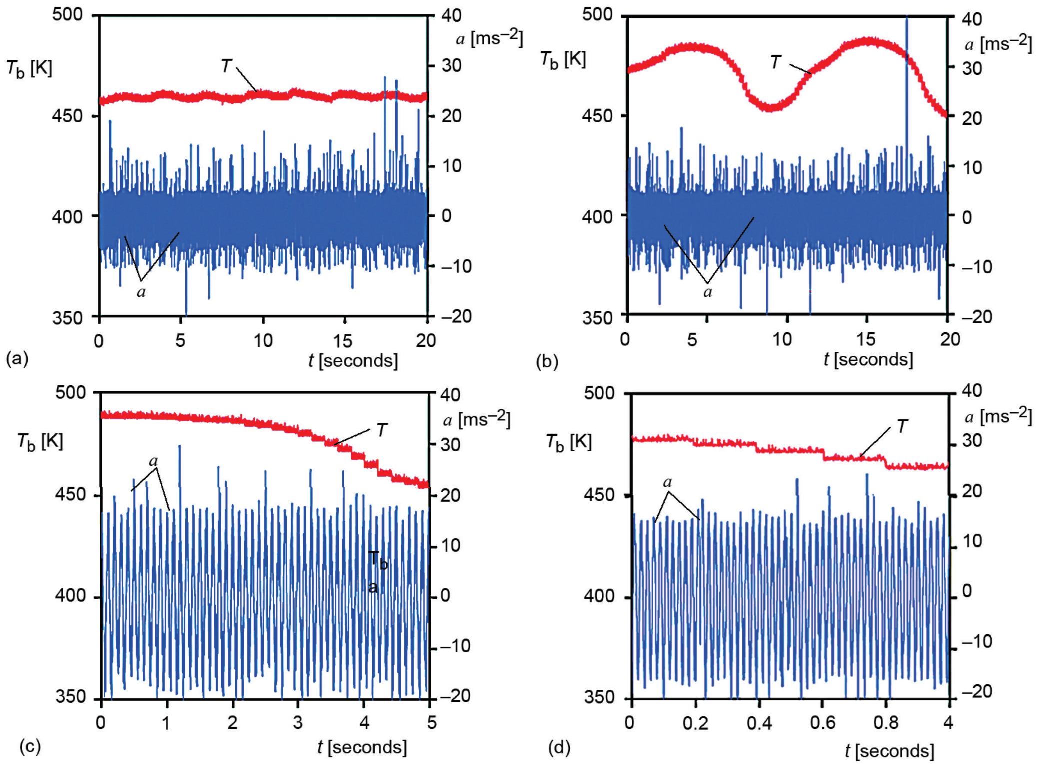

Figure 10. Four stages of boiling oscillation; (a) phase a, (b) phase b, (c) phase c, and (d) phase d

The outlet fuel temperature at the three moments of A, B, and C can reflect the oscillation information of the fuel temperature in one cycle, and fig. 11 depicts the value of the outlet fuel temperature during the boiling oscillation. When external vibrations with a frequency of 10 Hz and vibration acceleration of 20 m/s^2 or those with a frequency of 50 Hz and vibration acceleration of 20 m/s^2 are applied to the pipe, the dynamic process of the influence of external vibration on the thermoacoustic oscillation in a cycle can be studied by the downstream fuel temperature at A, B, and C.

The variation in the inner wall temperature along the flow direction is shown in fig. 12. It can be clearly found that the external vibration has a greater impact on the inner wall temperature, when the fuel is in the liquid state, the external vibration leads to a small increase in the wall temperature, when the fuel is in zone I and zone II, the external vibration obviously leads to a decrease in the temperature of the inner wall, in the zone III and single-phase gas state, the external vibration has little effect on the inner wall temperature. Figure 13 depicts the change of the mainstream temperature along the flow direction, and it is found that the mainstream temperature has almost no effect, so the effect on the mainstream thermophysical properties is small.

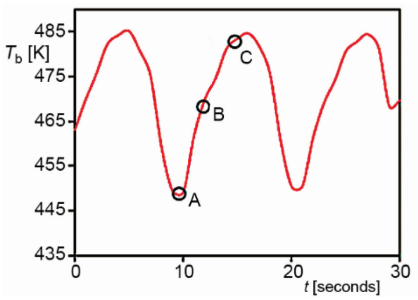

Figure 11. Exit fuel temperature of boiling oscillation

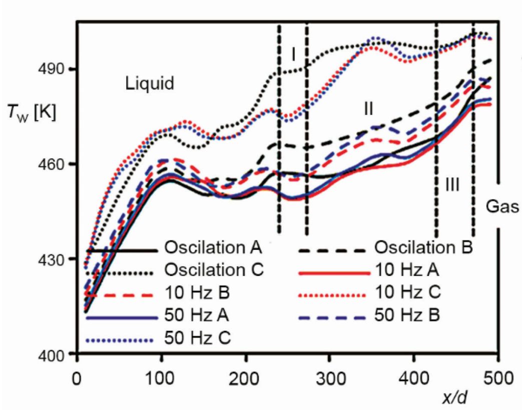

Figure 12. Variations of inner wall temperature

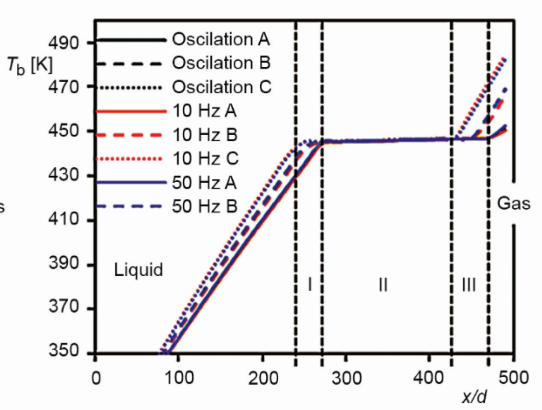

Figure 13. Variations of fuel temperature along

The influence of external vibration on the boiling oscillation heat transfer coefficient is shown in fig. 14, when the fuel is in a single-phase liquid state, the heat transfer coefficient curves are basically coincide with or without the external vibration, indicating that the external vibration has no effect on the heat transfer in this area. In Zone I, the fuel constantly changes between the liquid state and the boiling state, and external vibration causes a sharp increase in the heat transfer coefficient, reaching a peak when all fuel is about to enter a boiling state.

In Zone II, the heat transfer coefficient under vibration conditions decreases rapidly, and at about x/d = 340, the heat transfer coefficient under external vibration conditions basically coincides with the heat transfer coefficient under no vibration conditions. In summary, vibration mainly affects the boundary of Zones I and II, reducing the wall temperature and thus improving heat transfer. As can be seen from the distribution of Reynolds number along the course in fig. 15, the variation in the flow state is small.

Influence of vibration on unstable heat transfer at quasi-critical pressure

At quasi-critical pressure (3 MPa), it was found in the experiment that every time the system screamed, the radial acceleration sensor of the pipeline would have a pulse signal, and its acceleration peak was in the range of 100 m/s^2 to 400 m/s^2. With each abrupt change in acceleration, the fuel temperature will suddenly increase by about 70 K. As shown in

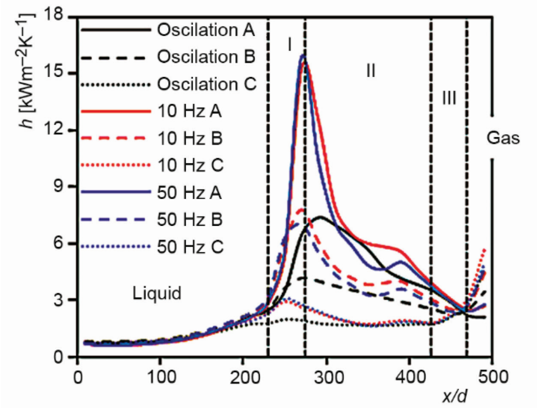

Figure 14. Variations of heat transfer coefficient

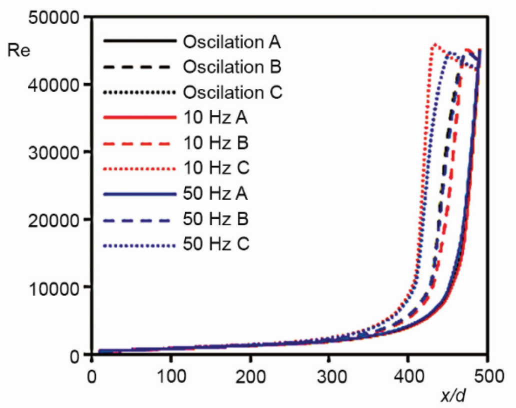

Figure 15. Variations of Reynolds number

fig. 16(a), where Phase a is the thermoacoustic oscillation stage and there is no external vibration, Phase b is the thermoacoustic oscillation stage, and the pipe is subjected to radial vibrations with a frequency of 10 Hz and an amplitude of 20 m/s^2, Phase c is the thermoacoustic oscillation stage, and the pipe is subjected to radial vibrations with a frequency of 50 Hz and an

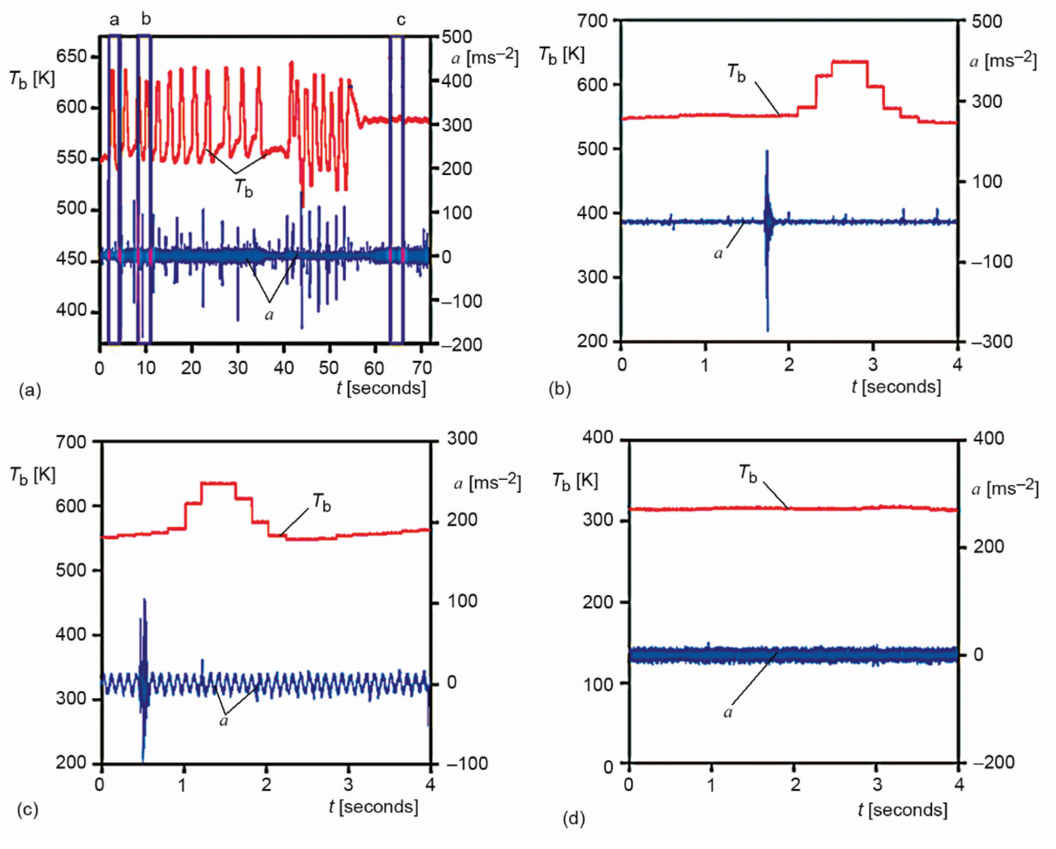

Figure 16. The unsteady flow under quasi-critical pressure condition; (a) outlet fuel temperature, (b) Phase a, (c) Phase b, and (d) Phase c

amplitude of 20 m/s^2. As shown in fig. 17(b), when thermoacoustic oscillation occurs, the pipe is first subjected to an acceleration pulse, and then the fuel temperature begins to oscillate, indicating that the oscillation of the fuel temperature is affected by the sound pulsation. The temporal relationship between the acceleration information and the fuel temperature information in fig. 17(c) also exists in this phenomenon. The radial vibration with a frequency of 10 Hz and an amplitude of 20 m/s^2 did not change the process of thermoacoustic oscillation. The value of the fluctuating temperature and acceleration pulse of the fuel did not change significantly. As shown in fig. 17(d), when the vibration amplitude is assured, but the vibration frequency reaches 50 Hz, the thermoacoustic oscillation phenomenon disappears, which is manifested in the disappearance of the acceleration pulse and the absence of fluctuations in the fuel.

The A and B represent the peak and trough positions of the fuel oscillation, which can reflect the oscillation information of the fuel temperature in one cycle, and fig. 17 depicts the value of the outlet fuel temperature during thermoacous oscillation under quasi-critical pressure. When the external vibration is applied to the pipe at a frequency of 10 Hz, an amplitude of 20 m/s^2, and a frequency of 50 Hz, an amplitude of 20 m/s^2, the dynamic process of the influence of external vibration on boiling oscillation in a cycle can be studied by the distribution patterns of fuel temperature, temperature of the inner wall, heat transfer coefficient, and Reynolds number along the length at A and B.

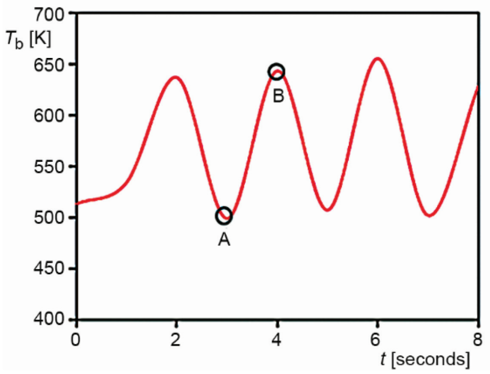

Figure 17. Exit fuel temperature of boiling oscillation

The variation of the inner wall temperature along the flow direction is shown in fig. 18. It is found that the external vibration has a significant impact on the near wall surface, when x/d < 200, the external vibration causes the inner wall temperature to rise, the greater the frequency, the greater the amplitude of the rise, the greater the acceleration amplitude, the smaller the increase, and the influence of the frequency is significantly greater than the impact of the acceleration amplitude. When 200 < x/d < 300, the wall temperature under external vibration conditions is the same as the temperature without vibration. When x/d > 200, the external vibration again causes the temperature of the inner wall to rise, and its influence law is basically the same as that of x/d < 200. Figure 19 depicts the variation of the mainstream temperature along the flow direction, and finds that the amplitude of the fuel temperature fluctuation increases linearly along the flow direction. The oscillation amplitude of the mainstream temperature decreases significantly during external vibrations, and the oscillation amplitude of 50 Hz is less than the oscillation amplitude of 10 Hz.

The influence of external vibration on the boiling oscillation heat transfer coefficient is shown in fig. 20. When there is no external vibration, the heat transfer process of the thermal acoustic oscillation changes very dramatically, which is caused by a large oscillation of the fuel temperature. The variation in the heat transfer coefficient with external vibration decreases because the amplitude of the oscillation of the fuel temperature decreases significantly and the wall temperature rises by a small margin. As can be seen from fig. 21, no vibration and 10 Hz vibration at the outlet will cause the phenomenon of strong turbulence, while 50 Hz vibration will cause the flow regime of the outlet to change, and the variation in the flow state will also lead to a non-linear change in the heat transfer coefficient in the outlet section.

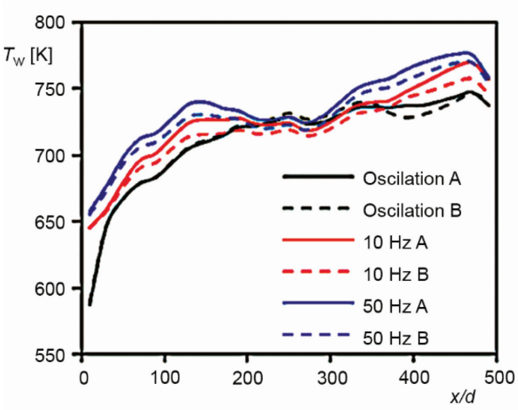

Figure 18. Variations of inner wall temperature

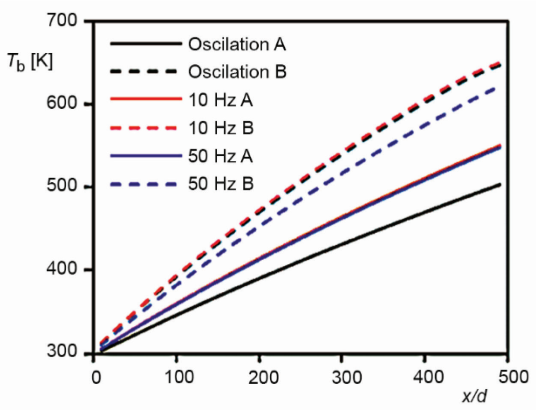

Figure 19. Variations of fuel temperature along

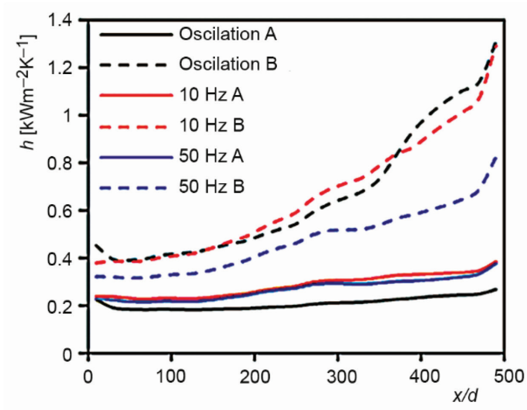

Figure 20. Variations of inner wall temperature

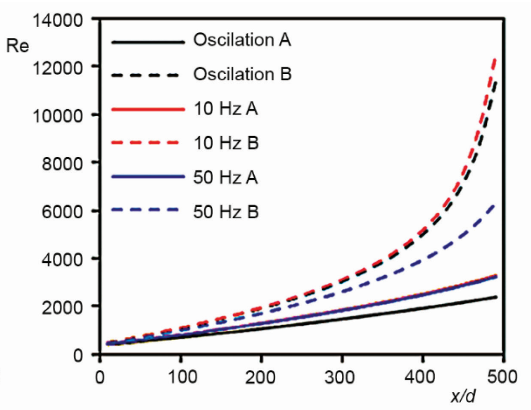

Figure 21. Variations of fuel temperature

Conclusions

In this paper, the influence of external vibration on heat transfer in hot-end channel flow under quasi-critical pressure is taken as the guidance. Firstly, the influence of external vibration on the heat transfer of stable flow in hot-end channel is studied, and then the influence of external vibration on the heat transfer of unstable flow induced by heat flow in high temperature channel is studied. The conclusions are as follows.

- At atmospheric pressure, cooling channel vibration causes a drastic change in the temperature of the inner wall during unstable heat transfer process, but vibration will not change the fuel bulk temperature oscillation process. As a result, forced vibration can lead to deterioration of heat transfer in the gas-liquid two-phase flow.
- Unlike atmospheric pressure condition, cooling channel vibration not only change the inner wall temperature, but also influence fuel bulk temperature quasi-critical pressure. The forced vibration can lead to heat transfer enhancement. High frequency vibration will suppress heat transfer instability and reduces heat transfer fluctuations.

References

[1] Zhang, J. L., *et al.*, Investigations on Flame Liftoff Characteristics in Liquid-Kerosene Fueled Supersonic Combustor Equipped with Thin Strut, *Aerospace Science and Technology, 84* (2019), Jan., pp. 686-697

[2] Chen, M., *et al.*, Study on Influence of Forced Vibration of Cooling Channel on Flow and Heat Transfer of Hydrocarbon Fuel at Supercritical Pressure, *Thermal Science, 26* (2022), 4B, pp. 3463-3476

[3] Majdak, M., *et al.*, Analysis of Thermal Flow in Waterwall Tubes of the Combustion Chamber Depending on the Fluid Parameters, *Thermal Science, 23* (2019), Suppl. 4, pp. S1333-S1344

[4] Linne, D. L., *et al.*, Investigation of Instabilities and Heat Transfer Phenomena in Supercritical Fuels at High Heat Flux and Temperatures, *AIAA Paper*, (2000), Aug., pp. 2000-3128

[5] Zan, H., *et al.*, Recurrence Network Analysis for Uncovering Dynamic Transition of Thermo-Acoustic Instability of Supercritical Hydrocarbon Fuel Flow, *Aerospace Science and Technology, 85* (2019), Feb., pp. 1-12

[6] Qin, J., *et al.*, Experimental Study on Chemical Recuperation Process of Endothermic Hydrocarbon Fuel, *Fuel, 108* (2013), 11, pp. 445-450

[7] Jovanović, M. M., *et al.*, Rayleigh-Benard Convection Instability in the Presence of Temperature Variation at the Lower Wall, *Thermal science, 16* (2012), 2, pp. 281-294

[8] Yang, S., *et al.*, A New Cognition on Oscillatory Thermocapillary Convection for High Prandtl Number Fluids, *Thermal Science, 25* (2021), 6B, pp. 4761-4772

[9] Kafengauz, N. L., *et al.*, Pseudoboiling and Heat Transfer in a Turbulent Flow, *Journal of Engineering Physics, 14* (1968), 5, pp. 489-490

[10] Linne, D. L., *et al.*, Evaluation of Heat Transfer and Thermal Stability of Supercritical JP-7 Fuel, *AIAA Paper, 3041,* 33rd Joint Propulsion Con. and Exibit., Seattle, Wash., USA, 1997

[11] Alad'Ev, I T., *et al.*, Characteristics of Self-Excited Thermoacoustic Oscillations In Heat Transfer to N-Heptane, *Journal of Engineering Physics and Thermophysics, 33* (1977), 1, pp. 752-755

[12] Hitch, B., *et al.*, Enhancement of Heat Transfer and Elimination of Flow Oscillations in Supercritical Fuels, *AIAA Paper*, *3759,* 34rd Joint Propulsion Con. and Exibit., Clevland, O., USA, 1998

[13] Hitch, B., *et al.*, Experimental Investigation of Heat Transfer and Flow Instabilities in Supercritical Fuels, *AIAA Paper*, *3043,* 33rd Joint Propulsion Con. And Exibit., Aeattle, Wash., USA, 1997

[14] Zhu, Y. H., *et al.*, Investigation of Flow and Heat Transfer Instabilities and Oscillation Inhibition of N-Decane at Supercritical Pressure in Vertical Pipe, *Applied Thermal Engineering, 161* (2019), 7, 114143

[15] Edwards, T., USAF Supercritical Hydrocarbon Fuels Interests, *AIAA Paper*, *0807,* 31st Aerospace Sci. Meeting, Reno, Nev., USA, 1993

[16] Hines, W. S., *et al.*, Pressure Oscillations Associated with Heat Transfer to Hydrocarbon Fluids at Supercritical Pressures and Temperatures, *ARS Journal, 32* (1962), 3, pp. 361-366

[17] Liu, Z., *et al.*, Convective Heat Transfer and Pressure Drop Characteristics of Near-Critical-Pressure Hydrocarbon Fuel in a Minichannel*, Applied Thermal Engineering, 51* (2013), 1-2, pp. 1047-1054

[18] Zhou, W., *et al.*, Mechanism and Influencing Factors Analysis of Flowing Instability of Supercritical Endothermic Hydrocarbon Fuel within a Small-Scale Channel, *Applied Thermal Engineering, 71* (2014), 1, pp. 34-42

[19] Wang, H., *et al.*, Experimental Investigation on the Onset of Thermo-Acoustic Instability of Supercritical Hydrocarbon Fuel Flowing in a Small-Scale Channel, *Acta Astronaut, 117* (2015), Dec., pp. 296-304

[20] Wang, H., *et al.*, Experimental Investigation on the Characteristics of Thermo-Acoustic Instability in Hydrocarbon Fuel at Supercritical Pressures, *Acta Astronaut, 121* (2016), Apr., pp. 29-38

[21] Han, Y., *et al.*, Assessment of a Hybrid RANS/LES Simulation Method and URANS Method in Depicting the Unsteady Motions of Flow Structures in a Scramjet Combustor, *Aerospace Science and Technology, 72* (2018), Jan., pp. 114-122

[22] Ma, F., *et al.*, Thermoacoustic Flow Instability in a Scramjet Combustor, *AIAA Paper*, *3824*, 41st Join Propulsion Con. and Exhibit. Tucson, Ariz., USA, 2005

[23] Katinas, V. I., *et al.*, Heat Transfer Behavior of Vibrating Tubes Operating in Crossflow. 1. temperature and Velocity Fluctuations, *Heat Transfer-Soviet Research, 18* (1986), 2, pp. 1-9

[24] Cheng, C. H., *et al.*, Experimental Study of the Effect of Transverse Oscillation on Convection Heat Transfer from a Circular Cylinder, *Journal of Heat Transfer, 119* (1997), 3, pp. 474-482

[25] Deng, H. W., *et al.*, Density Measurements of Endothermic Hydrocarbon Fuel at Sub- and Supercritical Conditions, *Journal of Chemical and Engineering Data, 56* (2011), 6, pp. 2980-2986

Paper submitted: September 18, 2022
Paper revised: December 8, 2022
Paper accepted: December 12, 2022